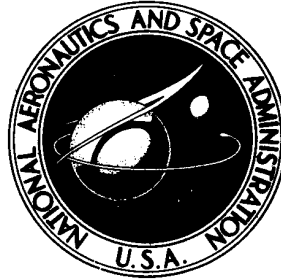


**NASA TECHNICAL NOTE**



**NASA TN D-8216**

**NASA TN D-8216**

**EVALUATION OF AN ENVELOPE-LIMITING DEVICE  
USING SIMULATION AND FLIGHT TEST  
OF A REMOTELY PILOTED RESEARCH VEHICLE**

*Kevin L. Petersen*

*Dryden Flight Research Center  
Edwards, Calif. 93523*



**NATIONAL AERONAUTICS AND SPACE ADMINISTRATION • WASHINGTON, D. C. • APRIL 1976**



EVALUATION OF AN ENVELOPE-LIMITING DEVICE  
USING SIMULATION AND FLIGHT TEST OF A  
REMOTELY PILOTED RESEARCH VEHICLE

Kevin L. Petersen  
Dryden Flight Research Center

SUMMARY

The operational characteristics of a nonlinear envelope-limiting device at extreme flight conditions were evaluated. A digital mechanization of the F-15 control system, which included a stall inhibitor, was implemented for a 3/8-scale model F-15 remotely piloted research vehicle (RPRV). The stall inhibitor effectively increased the back stick force necessary for high angle of attack maneuvering and decreased the spin susceptibility of the airplane. A real time digital aircraft simulation, along with flight tests of the scale model using the RPRV technique, was found to constitute an effective evaluation method.

INTRODUCTION

Trends in recent aircraft control system designs indicate continuing interest in various types of envelope-limiting devices. These nonlinear control devices include hard and soft boundary limiters for various aircraft parameters, such as angle of attack, velocity, and normal acceleration; departure preventers; and stall inhibitors (refs. 1 and 2). The control augmentation system of the F-15 airplane has a nonlinear control schedule based on angle of attack, designated a stall inhibitor. A 3/8-scale remotely piloted research vehicle (RPRV) used for high angle of attack and spin research allowed this device to be investigated in flight.

A digital representation of the full-scale control system was mechanized for the RPRV and flight tested at the Dryden Flight Research Center. Reference 3 gives a description of the RPRV technique and an analysis of the scale digital control system. This report describes an evaluation of the stall inhibitor mechanized for the RPRV, with emphasis on the operational characteristics of the stall inhibitor and the effects of the stall inhibitor on spin susceptibility. The stall inhibitor mechanization is typical of this class of envelope-limiting devices, although the stall inhibitor in the

F-15 airplane does not restrict the airplane's flight envelope. Most of the investigation was performed by using a real time digital simulation of the RPRV which included the digital mechanization of the control system. The simulation results were verified in flight tests of the model using the RPRV technique.

## SYMBOLS

$F_{\delta_h}$	longitudinal stick force, N
$q$	pitch rate, deg/sec
$q_{wo}$	washed-out pitch rate, deg/sec
$s$	Laplace transform variable
$\alpha$	angle of attack, deg
$\alpha'$	stall inhibitor schedule command, deg
$\delta_{a_s}$	lateral stick deflection, positive right, cm
$\delta_h$	total stabilator command, positive trailing edge down, deg
$\delta_{h_A}$	augmented stabilator command, deg
$\delta_{h_B}$	basic stabilator command, deg
$\delta_{h_{SI}}$	stall inhibitor command, deg
$\delta_{h_s}$	longitudinal stick deflection, positive rearwards, cm
$\delta_{h_T}$	longitudinal trim command, cm

## ABBREVIATIONS

CAS	control augmentation system
MCS	mechanical control system
RPRV	remotely piloted research vehicle

## REMOTELY PILOTED RESEARCH VEHICLE TECHNIQUE

The RPRV technique evolved as a result of an effort to develop a low-cost supplement to full-scale manned flight testing for high risk flight tests that included stalls and spins. The technique provides the pilot with full closed-loop control of the flight test vehicle from a ground-based cockpit, eliminating the risk to the pilot. A diagram of the RPRV technique, which includes a ground-based RPRV facility, is shown in figure 1. The implementation of the RPRV technique is enhanced greatly by the use of a real time digital simulation of the RPRV system.

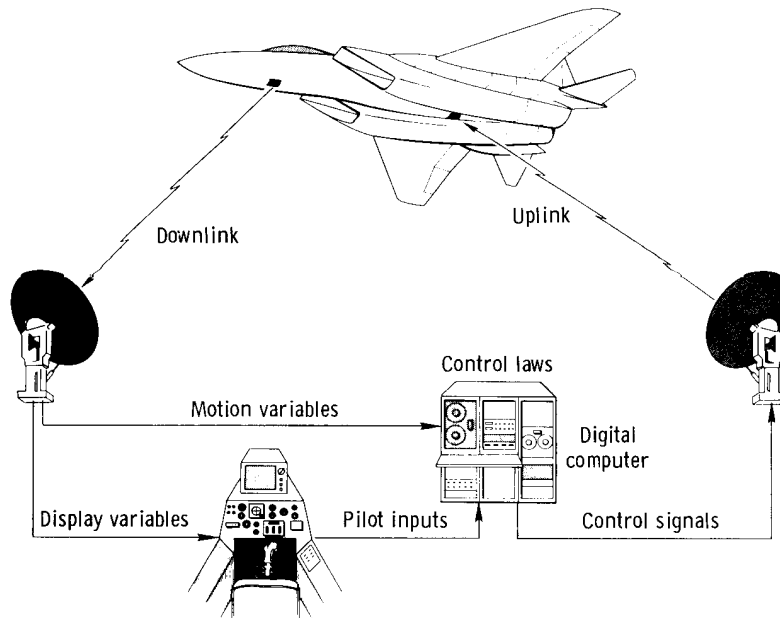


*Figure 1. Remotely piloted research vehicle technique.*

### Remotely Piloted Research Vehicle Facility

As illustrated in figure 1, the RPRV facility includes a telemetry transmitter for the uplink, a receiver for the downlink, a ground-based cockpit, and a ground-based digital computer. The ground-based digital computer, which provides closed-loop control law computation, is the key to the RPRV control system. Vehicle motion parameters are transmitted to the ground by the telemetry downlink. Instrument display variables are sent to the ground cockpit, from which the pilot makes control inputs to the ground-based digital computer. The inputs, along with the feedback response variables, are processed in the ground-based computer, and the surface commands are transmitted to the vehicle through a telemetry uplink. A more detailed description of the RPRV facility is given in reference 3.

## Model and Control System

A three-view drawing of the 3/8-scale model of the F-15 airplane is shown in figure 2. The control surfaces consist of left and right stabilators for pitch and roll control, ailerons for roll control, and twin rudders for yaw control. The inertial-force-to-gravity-force scaling technique was used to scale the model, which is unpowered. The model and the scaling techniques used are described in more detail in reference 3.

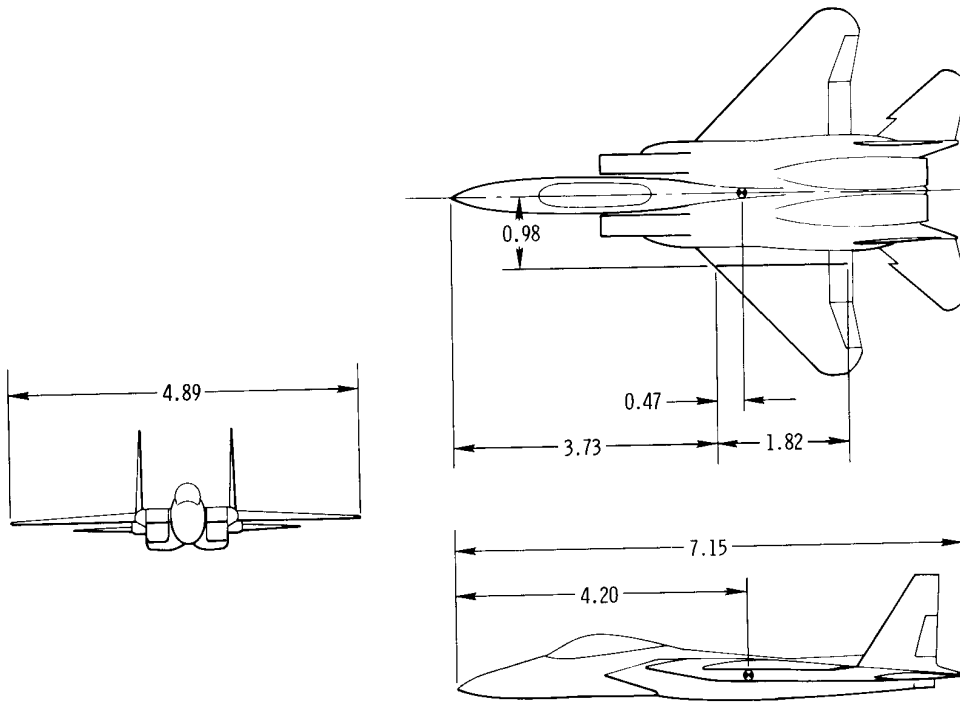


*Figure 2. Three-view drawing of 3/8-scale F-15 model. Dimensions in meters.*

Representations of the full-scale airplane's basic open-loop mechanical control system (MCS) and closed-loop feedback control augmentation system (CAS) were digitally mechanized in the ground-based computer. The digital mechanization included actuator dynamics, gearing schedules, gains, filters, and such nonlinear functions as the stall inhibitor. To insure the proper simulation of the full-scale control system, all control system gains and characteristic frequencies were scaled appropriately. Because of the inherent low-speed operating envelope of the unpowered model and the scaling technique used, the velocity-dependent schedules of the full-scale control system were not simulated.

The CAS operates on five feedback variables (pitch rate, roll rate, yaw rate, normal acceleration, and lateral acceleration) and uses angle of attack for scheduling purposes. The CAS is programmed to downmode to the MCS automatically when a predetermined yaw rate is exceeded. The MCS has less surface authority than the CAS in the longitudinal as well as in the lateral and directional axes. The operating characteristics of the MCS and the CAS are described in reference 3.

### Real Time Digital Simulation Facility

A simulation of the RPRV system was necessary to check out the computer program and to provide pilot training and flight planning capability. The basic aircraft simulation included six-degree-of-freedom equations of motion, which were mechanized on the Dryden Flight Research Center's central computer, utilizing its real time simulation capability. A second-order Runge-Kutta integration technique was used to integrate the airplane's continuous differential equations of motion numerically. Wind-tunnel aerodynamic force and moment data, updated with flight test results, were used in the simulation. No small angle approximations were assumed. To make it possible to simulate the stalling and spinning maneuvers made during the model flight tests, wind-tunnel aerodynamic data for angles of attack from  $0^\circ$  to  $90^\circ$  and angles of sideslip from  $-40^\circ$  to  $40^\circ$  were incorporated in the simulation.

The MCS and CAS were simulated in addition to the basic aircraft. An all-digital representation of the full-scale analog control system, including scaling effects, was created, and it was implemented in both the central digital computer used for the simulation and the ground-based digital computer used for the RPRV flight tests. The digital filters and actuator dynamics required were implemented by difference equations that were updated at the rate at which the RPRV system operated; therefore, the processing of the control system difference equations simulated the operational characteristics of the RPRV computer.

The simulator proved to be a valuable tool in evaluating the operational characteristics of the stall inhibitor. Confidence in the simulation increased throughout the flight program: the simulator-developed forced spin entries proved to be effective in actual flight (ref. 4), and the simulation data correlated well with the flight data (ref. 3).

### DESCRIPTION OF STALL INHIBITER

Figure 3 is a functional diagram of the full-scale longitudinal control system, including the stall inhibitor. The total stabilator command,  $\delta_{h_A}$ , is a combination of the basic stabilator command,  $\delta_{h_B}$ , and the commands originating from the CAS,

$\delta_{h_A}$  and  $\delta_{h_{SI}}$ . The command that originates from the MCS,  $\delta_{h_B}$ , is also used as the basis for the lateral and directional control system schedules. (The lateral and directional system schedules are designed on the basis of stabilator position but are

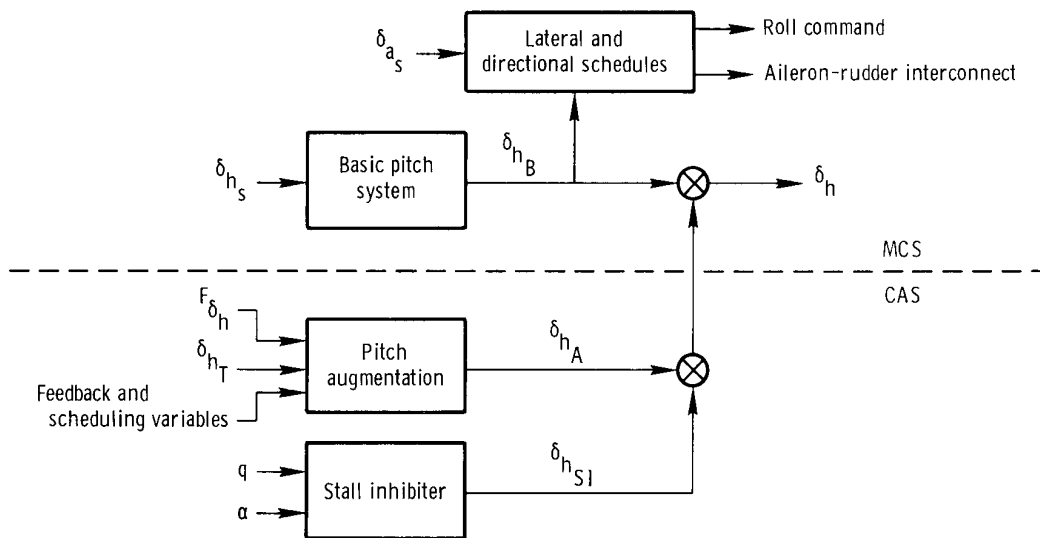


Figure 3. Control system.

scheduled with the basic stabilator command of the MCS.) The design intent of the stall inhibitor is to counteract the contribution of  $\delta_{h_A}$  to the total stabilator command at high angles of attack. By effectively washing out the contribution of the pitch CAS to  $\delta_h$  at high angles of attack, the stall inhibitor forces  $\delta_h$  to approximate  $\delta_{h_B}$ . Therefore, the lateral and directional system schedules provide better approximations of the MCS control authority, and this improves the aircraft's roll coordination at high angles of attack.

The full-scale stall inhibitor (fig. 4) includes a washout filter for pitch rate and a nonlinear schedule which is a function of a combination of angle of attack and

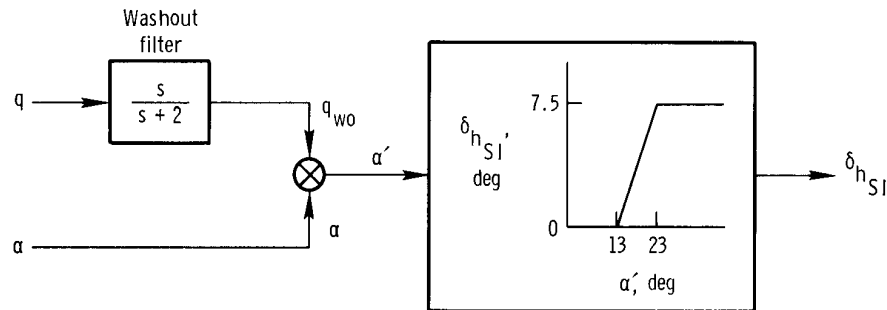


Figure 4. Stall inhibitor mechanization.



washed-out pitch rate. The stall inhibitor operates when the pitch CAS operates at high angles of attack, at high noseup pitch rates, or both. The combination of angle of attack and washed-out pitch rate forms the signal  $\alpha'$ , which is the basis of the stall inhibitor command schedule. This schedule determines the stall inhibitor command,  $\delta_{h_{SI}}$ , which produces a nosedown command when  $\alpha'$  exceeds  $13^\circ$ . The maximum

authority of the stall inhibitor is  $7.5^\circ$ . In the full-scale airplane, the stall inhibitor operates whenever the CAS is operating; however, the stall inhibitor mechanized in the RPRV could be activated or deactivated for test purposes. Therefore, when the stall inhibitor was inactive, the CAS mechanized for the RPRV differed from the CAS for the full-scale airplane.

## EVALUATION METHOD

The simulation was used to determine the effects of the stall inhibitor on the airplane's response. Time histories of various aircraft response parameters and surface positions were generated with the simulation, using the same initial conditions and pilot inputs for cases with and without the stall inhibitor. These time histories made possible direct comparisons between the simulated operational characteristics of the pitch CAS with and without the stall inhibitor operating. The simulation results were verified with flight results acquired with the model.

## SIMULATION STUDY

The simulator investigation included a determination of the static and dynamic effects of the stall inhibitor and the effects of the stall inhibitor on the tendency of the aircraft to spin.

### Static Effects of Stall Inhibiter

Figure 5 illustrates the operation of the pitch CAS with and without the stall inhibitor active for a simulated pullup maneuver performed on the simulator. The stick and force inputs for the maneuvers were identical. This figure, considered in conjunction with figure 3, illustrates the operation of the components of the pitch CAS mechanization during the maneuver. As angle of attack increases from  $13^\circ$  to  $23^\circ$ , the stall inhibitor command,  $\delta_{h_{SI}}$ , increases from  $0^\circ$  to  $7.5^\circ$ . Above

an angle of attack of  $23^\circ$ , the stall inhibitor command remains at  $7.5^\circ$ . The difference in the total stabilator command,  $\delta_h$ , with and without the stall inhibitor is due to the stall inhibitor only.

As shown in figure 3, the pitch CAS command uses longitudinal stick force,  $F_{\delta_h}$ , as an input; therefore, the net effect of the stall inhibitor is to increase the longitudinal stick force at high angles of attack. Figure 6, which is a crossplot of

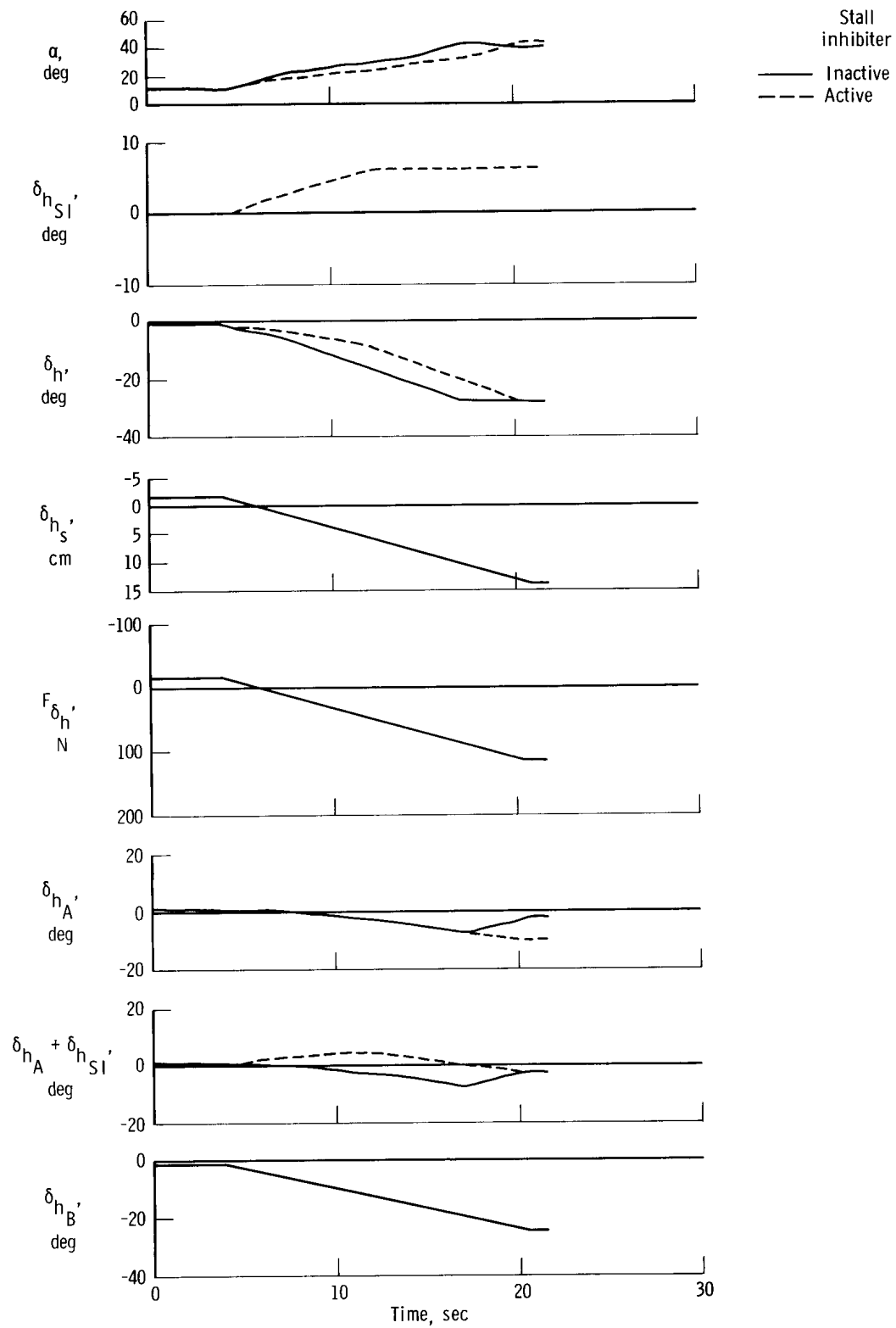


Figure 5. Operational characteristics of pitch CAS during a simulated pullup maneuver.

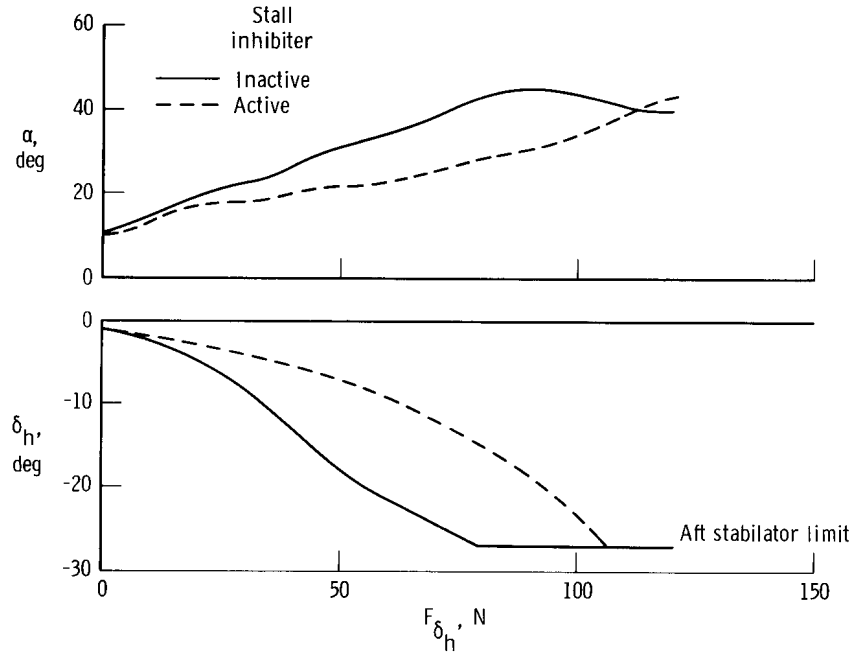


Figure 6. Effects of stall inhibitor on stick forces during pullup maneuver on simulator.

$\alpha$  and  $\delta_h$  as a function of  $F_{\delta_h}$ , indicates that to achieve comparable stabilator commands, and, correspondingly, comparable angles of attack, considerably more back stick force is required with the stall inhibitor active than inactive. The aft limit of the stabilator is eventually reached with the stall inhibitor active, indicating that the stall inhibitor can be overridden with increased back stick force. The need for increased back stick force when high angles of attack are approached serves to remind the pilot that the airplane is entering a high angle of attack region without limiting the flight envelope.

The stall inhibitor was intended to provide on-design lateral and directional control surface authority at high angles of attack to improve aircraft roll coordination in this region. To do so, the stall inhibitor command,  $\delta_{h_{SI}}$ , effectively counteracts the augmented stabilator command,  $\delta_{h_A}$ .

Ideally, the combination  $\delta_{h_A} + \delta_{h_{SI}}$  is zero in the high angle of attack region with the stall inhibitor operating.

Figure 7 is a plot of the pitch CAS command with the stall inhibitor operating,  $\delta_{h_A} + \delta_{h_{SI}}$ , as a function of angle of attack. Although  $\delta_{h_A} + \delta_{h_{SI}}$  differs from zero at all angles of attack, the stall inhibitor performs its intended function at the higher, more critical angles of attack.

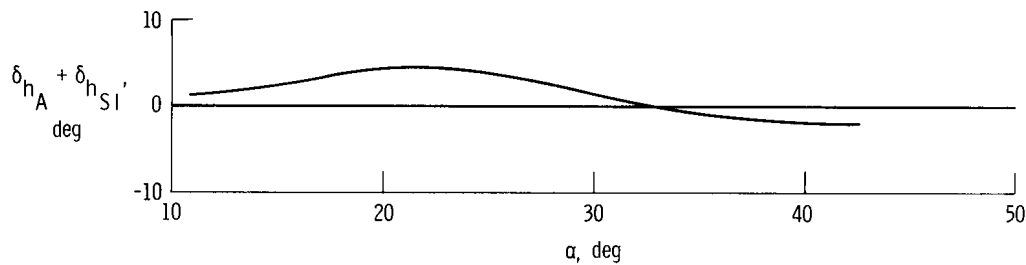


Figure 7. Pitch CAS command as a function of angle of attack.

### Dynamic Effects of Stall Inhibiter

The longitudinal dynamic effects of the stall inhibitor are primarily a result of the pitch rate input, which in effect provides an anticipatory term in the stall inhibitor mechanization. As shown in figure 4, pitch rate is processed through a wash-out filter and then combined with angle of attack to form the basis for the stall inhibitor command schedule. Sharp pitch rate and angle of attack inputs cause the stabilator to deflect sharply and result in short duration stabilator pulses. If the angle of attack is less than  $13^\circ$ , sharp pitch rate inputs cause positive stabilator deflections. If the angle of attack is between  $13^\circ$  and  $23^\circ$ , sharp pitch rate inputs cause stabilator deflections in either direction, depending on the sign of the pitch rate. If the angle of attack is greater than  $23^\circ$ , sharp pitch rate inputs cause only negative stabilator deflections, because at these angles of attack the  $7.5^\circ$  authority of the stall inhibitor is saturated.

### Effects of Stall Inhibiter on Spin Entries

The RPRV proved to be spin resistant in flight, so ways to force spin entries were developed on the simulator. A spin entry is a highly dynamic maneuver in which the cross coupling of the aircraft's lateral-directional and longitudinal dynamic characteristics force the airplane's angle of attack beyond the region of maximum lift while the airplane's yaw rate increases.

Three of the spin entries developed on the simulator were used in the flight tests. The first, referred to herein as the normal entry, is a 1g entry which involves applying full back stick until the angular rates stabilize. Then full lateral stick and opposite rudder controls are applied and back stick pressure is relieved to the neutral position. The second or high-g entry reaches approximately 4g. It involves pushing the vehicle over into a nearly vertical descent until a predetermined airspeed is obtained, applying full back and lateral stick with opposite rudder, and then relieving back stick pressure to a neutral condition. The third technique, called the slice entry technique, involves rolling the airplane  $90^\circ$  at low velocity and then allowing the airplane's nose to fall to a nearly vertical, nosedown

condition while keeping pitch and roll rates near zero. At that point opposite rudder and lateral stick inputs are made slowly and in a coordinated manner without the use of any longitudinal control. The slice spin entry was designed to minimize the effects of pitch rate on the stall inhibitor and therefore the spin entry. The final portion of all three spin entry techniques was identical—full lateral stick, full opposite rudder, and nearly neutral longitudinal stick. Since the longitudinal stick was nearly neutral in the critical portion of the spin entry, the lateral and directional surface authorities were the same with and without the stall inhibitor. Reference 4 gives a more detailed description of the three spin entries as well as a more complete explanation of the airplane's dynamic behavior during a spin.

A qualitative comparison of the spin susceptibility of the vehicle using these three entries was made on the simulator, and the results are presented in figure 8.

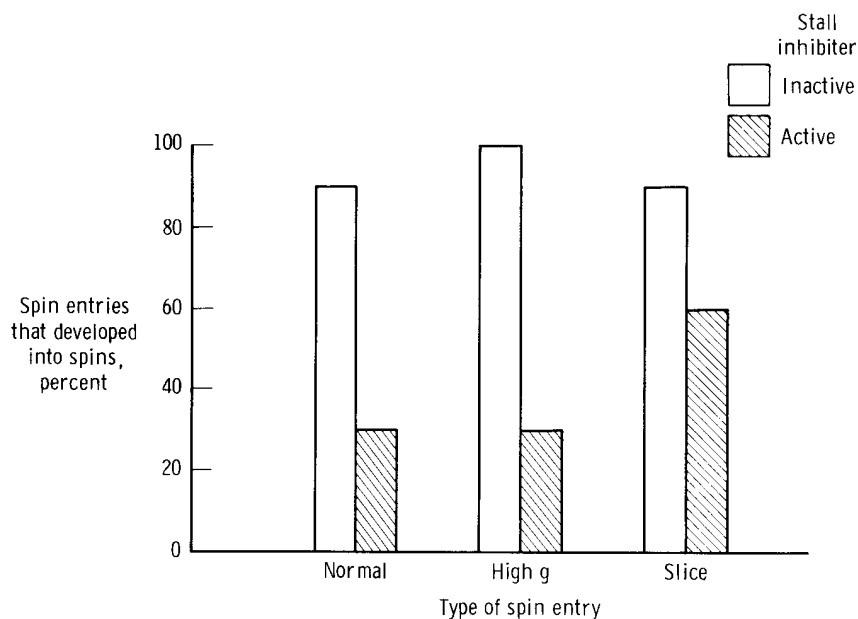


*Figure 8. Simulator comparison of three types of spin entries with and without stall inhibitor.*

For each of the three entries, 10 entry maneuvers were attempted with the stall inhibitor active and 10 were attempted with the stall inhibitor inactive. The attempts made with the stall inhibitor inactive produced developed spins nine out of 10 times for the normal and slice entries and 10 out of 10 times for the high-g entry technique. The attempts with the stall inhibitor active produced developed spins only three out of 10 times for the normal and high-g entries and six out of 10 times for the slice entry. It should be emphasized, however, that this simulator comparison is only qualitative.

The factor that seemed to govern whether or not the airplane would spin with the stall inhibitor active was the rate at which yaw rate increased relative to the activity of the stall inhibitor. An automatic downmode from the CAS to the MCS occurred when a predetermined yaw rate was exceeded. If the automatic downmode to the MCS occurred before the oscillations became too intense, the airplane usually entered the spin. However, the airplane often oscillated out of the spin entry if the oscillations encountered when the stall inhibitor was active were large.

Figure 9 illustrates a typical slice spin entry with and without the stall inhibitor. This simulator comparison was made by making identical pilot stick and force inputs at identical initial conditions; therefore, the difference in the airplane's behavior was due to the stall inhibitor. An airplane spin is commonly defined as a sustained oscillatory condition above the maximum lift angle of attack, which is approximately  $40^\circ$  for this airplane. As figure 9 shows, the entry with the stall inhibitor inactive developed into a spin, whereas the entry with the stall inhibitor active did not develop into a spin. The activity of the stall inhibitor is evident in the stabilator position, and the pulse in the stabilator position before the system downmodes to the MCS is characteristic.

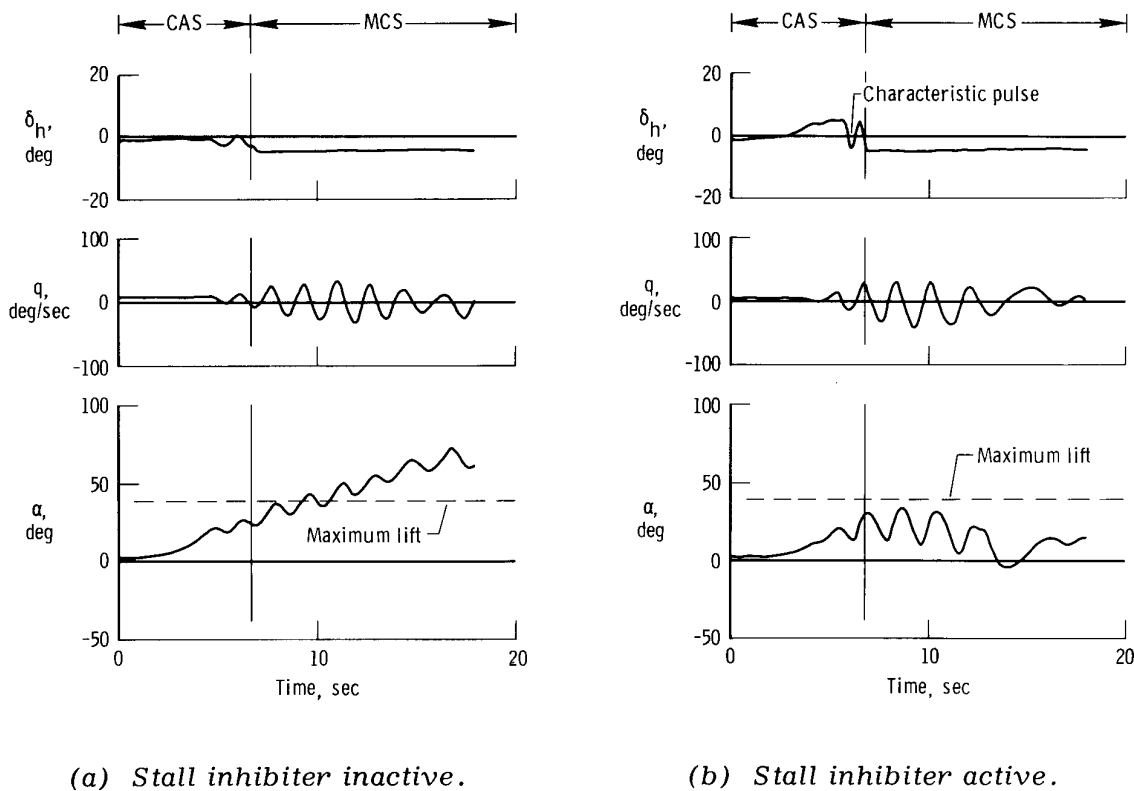


Figure 9. Simulator comparison of slice spin entry with and without stall inhibitor.

## FLIGHT EXPERIENCE

Flight tests were conducted with the RPRV with and without the stall inhibitor at altitudes from 15,250 meters to 4600 meters at Mach numbers below 0.6. The stall inhibitor was active during three spin entry attempts, none of which produced a spin. Two spin entries with the stall inhibitor active were attempted using the slice entry technique, which was designed to minimize pitch rate oscillations and therefore the effects of the stall inhibitor. The spin attempt shown in figure 10, which used this type of entry, illustrates the effects of the stall inhibitor. Since longitudinal stick was kept constant, the positive stabilator deflections were caused entirely by the stall inhibitor. As the angle of attack increased from  $13^\circ$  to  $23^\circ$ , the stabilator deflected in a positive direction, as expected. Above an angle of attack of  $23^\circ$ , the stabilator kept this position until the airplane became oscillatory enough to cause the stall inhibitor to produce the characteristic pulse in the stabilator. The CAS then downmoded to the MCS and the airplane oscillated out of the spin attempt and recovered.

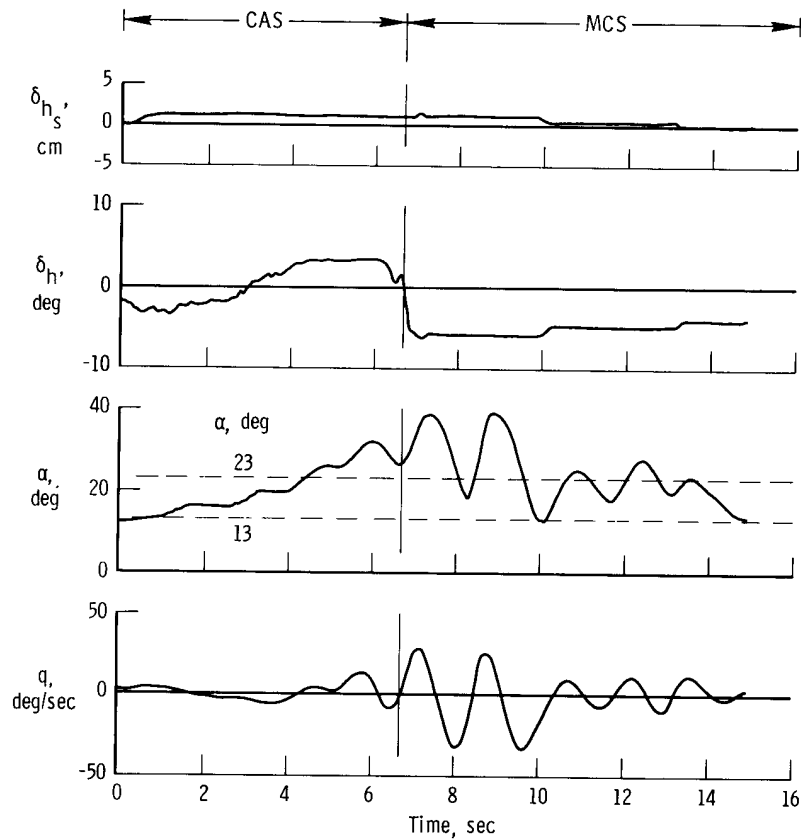
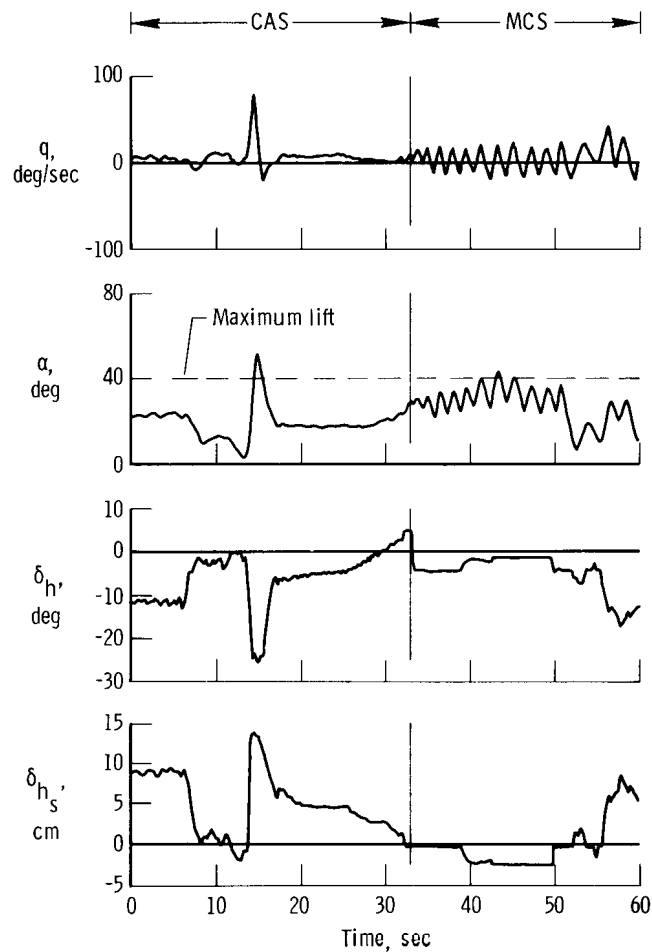


Figure 10. Flight time history of slice entry with stall inhibitor.

The high-g entry technique was used at a relatively low altitude for another attempt, and it did not produce a spin. During this entry attempt (fig. 11), pitch rate stabilized quickly; therefore, the contribution of pitch rate to the stall inhibitor



*Figure 11. Flight time history of high-g entry with stall inhibitor.*

was negligible. The effect of angle of attack on the stall inhibitor was to force a positive stabilator deflection that prevented the angle of attack from rising above the maximum lift point. When the CAS automatically downmoded to the MCS the angle of attack was still lower than the maximum lift point and the airplane did not enter a spin.

Figure 12 illustrates an attempt to spin the RPRV with the stall inhibitor inactive. This spin entry attempt, which was made with the high-g entry technique, was successful: The angle of attack proceeded beyond the maximum lift point and the airplane went into a sustained spin. A discussion of this spin and others produced with this and the other two spin entry techniques is given in reference 4, along



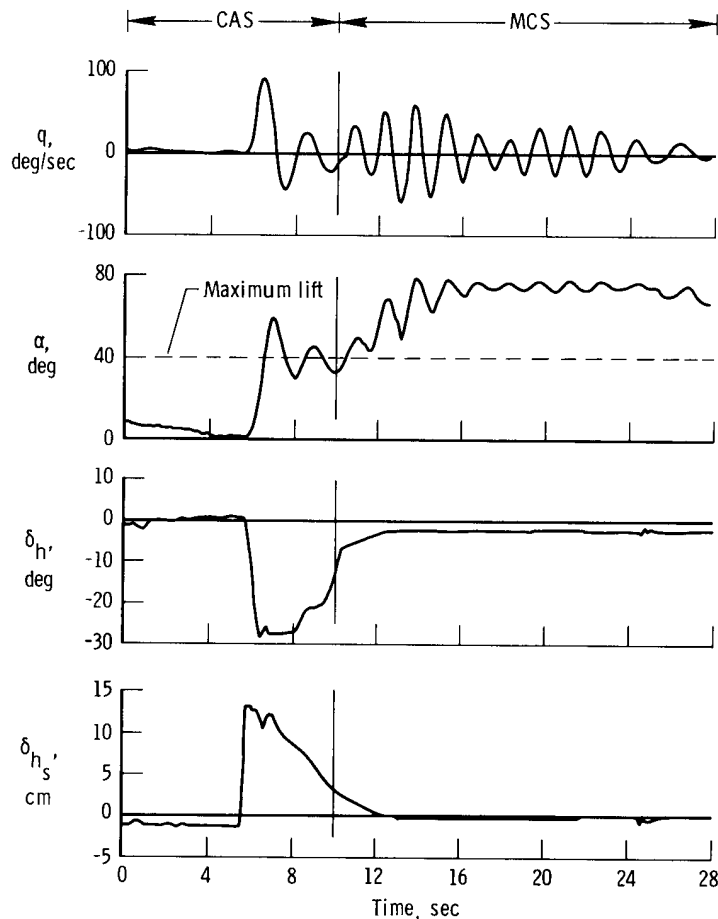


Figure 12. Flight time history of developed spin using high-g entry without stall inhibitor.

with complete descriptions of the maneuvers. Although too few tests were flown for trends like those in figure 8 to become apparent, the characteristics of the stall inhibitor and the subsequent behavior of the vehicle in flight were similar to those indicated by the simulator.

#### CONCLUDING REMARKS

The performance of the stall inhibitor of the F-15 control system was evaluated by using a real time digital aircraft simulation of a 3/8-scale model of the F-15 airplane and flight tests of the model using the remotely piloted research vehicle (RPRV) technique. Simulator-developed forced spin entries that usually produced aircraft spins when the stall inhibitor was inactive were less likely to produce spins when

the stall inhibitor was active. Flight tests verified the airplane's resistance to spinning with the stall inhibitor active.

The stall inhibitor reduced the airplane's spin susceptibility by producing positive stabilator deflections for specified angle of attack regions and by increasing the oscillatory behavior of the airplane during highly dynamic maneuvers. The stall inhibitor effectively increased the back stick forces necessary for high angle of attack maneuvering.

The full six-degree-of-freedom digital aircraft simulation, along with flights of the scale model using the RPRV technique, was an effective method for investigating the operating characteristics of an envelope-limiting device at extreme flight conditions.

*Dryden Flight Research Center  
National Aeronautics and Space Administration  
Edwards, Calif., December 3, 1975*

## REFERENCES

1. Lamers, John P.: Design for Departure Prevention in the YF-16. AIAA Paper No. 74-794, Aug. 1974.
2. Chen, Robert T. N.; Newell, Fred D.; and Schelhorn, Arno E.: Development and Evaluation of an Automatic Departure Prevention System and Stall Inhibiter for Fighter Aircraft. AFFDL-TR-73-29, Air Force Flight Dynamics Lab., Apr. 1973.
3. Edwards, John W.; and Deets, Dwain A.: Development of a Remote Digital Augmentation System and Application to a Remotely Piloted Research Vehicle. NASA TN D-7941, 1975.
4. Holleman, Euclid C.: Summary of Flight Tests To Determine the Spin and Controllability Characteristics of a Remotely Piloted, Large-Scale (3/8) Fighter Airplane Model. NASA TN D-8052, 1976.